ELSEVIER

Biochimica et Biophysica Acta 1513 (2001) 207–216

BIOCHIMICA ET BIOPHYSICA ACTA
BBA

www.bba-direct.com

In vitro and in vivo comparison of immunoliposomes made by conventional coupling techniques with those made by a new post-insertion approach

Debbie L. Iden, Theresa M. Allen *

Department of Pharmacology, University of Alberta, Edmonton, AB, Canada T6G 2H7

Received 2 March 2001; received in revised form 15 May 2001; accepted 15 May 2001

Abstract

Ligand-targeted liposomes have the potential to increase the therapeutic efficacy of antineoplastic agents. Recently, a combinatorial approach to the preparation of ligand-targeted liposomes has been developed, termed the post-insertion technique, which will facilitate the production of targeted liposomes. In this paper, Stealth immunoliposomes (SIL) coupled to anti-CD19 made by either a conventional coupling technique (SIL[anti-CD19]), or by the post-insertion technique (PIL[anti-CD19], were compared with respect to their in vitro binding and cytotoxicity and their ability to improve in vivo survival in tumor-bearing mice. The in vitro binding and uptake of PIL[anti-CD19] by CD19-expressing, B-cell lymphoma (Namalwa) cells was similar to that of SIL[anti-CD19] and both were significantly higher than binding of non-targeted liposomes (SL). In addition, no significant differences were found between the respective in vitro cytotoxicities of doxorubicin-loaded PIL[anti-CD19] or SIL[anti-CD19], or in their in vivo therapeutic efficacy in a murine model of human B-lymphoma. Overall, the results demonstrate that the post-insertion technique is a simple, flexible and effective means for preparing targeted liposomal drugs for clinical applications. © 2001 Elsevier Science B.V. All rights reserved.

Keywords: Immunoliposome; Anti-CD19; B-cell lymphoma; Doxorubicin; Targeted drug delivery system; Ligand-mediated targeting; Polyethylene glycol

Abbreviations: HSPC, hydrogenated soy phosphatidylcholine; mPEG-DSPE, polyethylene glycol (M_r 2000) covalently linked via a carbamate bond to distearoylphosphatidylethanolamine; CHOL, cholesterol; [^{3}H]CHE, cholesterol-[1,2-^{3}H-(*N*)]hexadecyl ether; NAM, *N*-acetylmethionine; MTT, 3-[4,5-dimethylthiazol-2-yl]-2,5-diphenyltetrazolium bromide; HEPES, 4-(2-hydroxyethyl)-1-piperazine ethanesulfonic acid; TI, tyraminylinulin; Mal-PEG-DSPE, maleimide-derivatized mPEG-DSPE; Hz-PEG-DSPE, hydrazide-derivatized mPEG-DSPE; SL, Stealth liposomes composed of HSPC:CHOL:mPEG-DSPE; SIL, preformed SL containing coupling lipids that were converted into Stealth immunoliposomes by coupling antibodies directly to the PEG terminus; IgG micelles, mPEG-DSPE micelles with antibodies coupled to the PEG terminus of the micelles; PIL, SL that were converted into immunoliposomes using the post-insertion technology from IgG micelles; DXR, doxorubicin; DXR-SL, SL loaded with DXR; DXR-SIL[anti-CD19], SIL coupled to anti-CD19 and loaded with DXR; DXR-PIL[anti-CD19], PIL containing anti-CD19 transferred into preformed DXR-loaded liposomes

* Corresponding author. Fax: +1-780-492-8078. *E-mail address:* terry.allen@ualberta.ca (Theresa M. Allen).

0005-2736/01/$ – see front matter © 2001 Elsevier Science B.V. All rights reserved.
PII: S0005-2736(01)00357-1

1. Introduction

Ligand-targeted liposomes are being researched for their ability to improve the selective toxicity of anticancer drugs, with the ultimate aim of improving the therapeutic efficacy and quality of life for cancer patients. Ligand-targeted liposomal anticancer drugs have been shown to have increased binding, improved cytotoxicities, and in many cases improved therapeutic efficacy, compared to non-targeted liposomes [1–10]. If ligand-targeted liposomes are to proceed to clinical trials, simple, flexible methods for their preparation need to be developed. A novel method to prepare ligand-targeted liposomes, termed the post-insertion technique, has recently been developed [11]. This method is a logical progression from the work of Uster et al. [12] and involves the coupling of ligands to the terminus of polyethylene glycol (PEG)-lipid derivatives in a micellar phase followed by the time- and temperature-dependent transfer of the ligand-coupled PEG-lipids into the bilayers of pre-formed, drug-loaded liposomes during a simple incubation step. This is appealing from a manufacturing point of view because a wide variety of ligands (including antibodies, antibody fragments, peptides, carbohydrates, etc.) could be easily inserted into liposomes containing any one of a wide variety of drugs (including those that have already been approved for clinical use, e.g. Caelyx® or Myocet®). It is also appealing from a clinical standpoint because post-insertion liposomes can be tailor-made to accommodate both the drug sensitivity of the particular malignancy and its receptor or antigen expression, leading to improvements in therapeutic effect.

Ishida et al. have previously shown that it is possible to prepare post-insertion immunoliposomes (PIL) that satisfy many of the established criteria for 'ideal immunoliposomes' [11,13]. The technique is simple, an appropriate level of stable ligand incorporation can be achieved, and the method does not compromise the drug-loading or drug release characteristics of doxorubicin-loaded liposomes [11]. In this paper the in vitro binding and cytotoxicity of immunoliposomes (PIL or Stealth immunoliposomes (SIL)) targeted with anti-CD19 monoclonal antibody were evaluated using a $CD19^+$ B-lymphoma cell line (Namalwa). The in vivo survival benefit of PIL was also evaluated and compared to that of SIL in a murine model of human B-cell lymphoma.

2. Materials and methods

2.1. Materials

Hydrogenated soy phosphatidylcholine (HSPC), methoxypoly(ethylene glycol) (MW 2000) covalently linked to distearoylphosphatidylethanolamine ($mPEG_{2000}$-DSPE) [14], hydrazide-derivatized PEG_{2000}-DSPE (Hz-PEG-DSPE) [15], and doxorubicin (DXR) were generous gifts from Alza Pharmaceuticals (Mountain View, CA). Maleimide-derivatized PEG_{2000}-DSPE (Mal-PEG-DSPE) was custom synthesized by Shearwater Polymers (Huntsville, AL). Cholesterol (CHOL) was purchased from Avanti Polar Lipids (Alabaster, AL). Cholesterol-[1,2-^{3}H-(*N*)]-hexadecyl ether ([^{3}H]CHE), 1.48–2.22 TBq/mmol, and $Na^{125}I$ (185 mBq) were purchased from Mandel Scientific (Mississauga, ON). [Carbamoyl-^{14}C]$mPEG_{2000}$-DSPE (17.75 mCi/g) was custom synthesized by Chemsyn Science Laboratories (Lenexa, KS). Nuclepore polycarbonate membranes (pore sizes: 0.2, 0.1, and 0.08 μm) were purchased from Northern Lipids (Vancouver, BC). Sephadex G-25 and G-50, Sepharose CL-4B, aqueous counting scintillant (ASC), and Hi-Trap protein G columns were purchased from Amersham Pharmacia Biotech (Baie d'Urfé, QC). *N*-Acetylmethionine (NAM), sodium periodate, 3-[4,5-dimethylthiazol-2-yl]-2,5-diphenyltetrazolium bromide (MTT), 2-iminothiolane (Traut's reagent), and sheep IgG (reagent grade) were purchased from Sigma (St. Louis, MO). 4-(2-Hydroxyethyl)-1-piperazine ethanesulfonic acid (HEPES) was purchased from BDH (Toronto, ON). Tyraminylinulin (TI) synthesis and preparation of [^{125}I]TI have been previously described [16]. RPMI 1640 medium (without phenol red), penicillin-streptomycin, and fetal bovine serum (FBS) were purchased from Life Technologies (Burlington, ON). All other chemicals were of analytical grade purity.

2.2. Cell lines and mice

The human Burkitt's lymphoma cell line, Namal-

wa (ATCC CRL 1432) (Rockville, MD) was grown in suspension at 37°C in 5% CO_2 and 90% humidity in full RPMI supplemented with 10% FBS, 50 units/ml penicillin G, and 50 μg/ml streptomycin sulfate. For experimental purposes, only cells in the exponential phase were used and CD19 expression was confirmed by flow cytometry [7].

Female, 6–8 week old Balb/C cr Alt BM mice were obtained from Health Sciences Lab Animal Services (University of Alberta, Edmonton, AB) and kept in standard housing. Female, 6–8 week old C.B.-17/ICR-Tac-SCID mice were purchased from Taconic Farms (German Town, NY) and housed under virus- and antigen-free conditions. They were fed autoclavable rodent chow and received trimethoprim-sulfamethoxazole in their drinking water. Both strains of mice were used for experiments after a minimum acclimation period of 1 week, when they were 7–12 weeks old. All experiments were approved by the Health Sciences Lab Animal Services Animal Policy and Welfare Committee of the University of Alberta.

2.3. Preparation of anti-CD19 antibody

Murine monoclonal anti-CD19 antibody (IgG2a) was produced in BALB/c cr Alt BM mice using the FMC63 murine hybridoma obtained from Dr. H. Zola, Children's Health Research Institute, Adelaide, Australia [17]. The antibody was purified from ascites fluid by centrifugation followed by filtration of the supernatant and purification on a protein G affinity column according to the manufacturer's instructions. A non-specific isotype-matched antibody that does not bind to Namalwa cell epitopes was obtained from the PK136 hybridoma (ATCC HB-191). Iodination of anti-CD19 was as previously described [7].

2.4. Preparation of liposomes

Non-targeted sterically stabilized liposomes (SL) were composed of HSPC:CHOL:$mPEG_{2000}$-DSPE at a 2:1:0.1 molar ratio. Targeted formulations were composed of 4 mol% $mPEG_{2000}$-DSPE and 1 mol% of coupling lipid (Mal-PEG_{2000}-DSPE [18] or Hz-PEG_{2000}-DSPE [7]). Formulations were made with either the anti-CD19 monoclonal antibody (mAb) or with an isotype-matched control antibody that did not bind to Namalwa cells. In some cases a non-metabolizable, non-exchangeable radioactive tracer, [^{3}H]CHE (30–60 kBq), was added to the lipid mix. Extrusion of the liposomes to homogeneous size was as previously described [7]. Briefly, dried lipid films were hydrated at a concentration of 20–30 mM phospholipid (PL) and sequentially extruded (Lipex Biomembranes Extruder, Vancouver, BC) through a series of polycarbonate membranes with pore sizes ranging from 0.2 μm down to 0.08 μm. The final liposome size was 100 ± 10 nm with a polydispersity ranging from 0.08 to 0.12. Liposomes for binding assays were hydrated in HEPES buffer, pH 7.4. When doxorubicin-loaded liposomes were required for in vitro cytotoxicity and in vivo therapeutic studies, the lipid was hydrated in 250 mM ammonium sulfate at pH 5.5.

For doxorubicin loading the liposome external buffer was exchanged for 100 mM Na acetate, 70 mM NaCl at pH 5.5 by chromatography on a CL-4B column and DXR was loaded by the ammonium sulfate gradient method [19] at a ratio of 0.2:1, DXR:HSPC (w/w) as previously described [20]. The DXR concentration was determined by spectrophotometry ($\lambda = 450$ nm) from the absorbance of the loaded liposomes dissolved in methanol and the phospholipid concentration was determined by the Bartlett colorimetric assay [21]. The final loading ratio was approx. 0.26 μmol DXR/μmol PL, which translates into approx. 99% loading efficiency.

2.5. Preparation of micelles

Lipid mixtures, composed of Mal-PEG_{2000}-DSPE and $mPEG_{2000}$-DSPE at a 4:1 molar ratio, were dried from chloroform for 1 h using a rotor-evaporator, then overnight under high vacuum. The lipids were hydrated immediately before coupling at a concentration of 10 mM in deoxygenated 25 mM HEPES, pH 7.4, by heating in a 65°C water bath with occasional gentle vortexing.

2.6. Antibody coupling to liposomes or micelles

Antibodies were usually coupled to the PEG termini of liposomes or micelles using the Mal-PEG coupling method [18]. The method was modified

for the coupling of whole antibody as described by Lopes de Menezes et al. [22]. For coupling to micelles, the antibody was thiolated at an antibody concentration of 12 mg/ml and a ratio of Traut's:IgG of 10:1 (mol/mol). The thiolated antibody was then promptly added to the liposomes or micelles at a specified molar ratio of IgG:PEG_{2000}-DSPE, taking care to avoid exposure to oxygen. For coupling to liposomes, approx. 45 μg Ab was added per μmol PL, which corresponds to a molar ratio of 1:3333 (Ab:liposome PL). Micelles were coupled at a molar ratio of 10:1, Mal-PEG_{2000}-DSPE:IgG.

2.7. Transfer of antibodies from micelles to liposomes

Following coupling, the IgG micelles were filtered through a 0.22 μm filter to remove any micelle aggregates that might have resulted from cross-linking. Micelles were then incubated with pre-formed liposomes containing 4 mol% PEG at a molar ratio of 0.05:1 (micelle PL:liposomal HSPC) for 1 h at 60°C. Following transfer, the liposome–micelle mixture was cooled and chromatographed over a Sepharose CL-4B column, equilibrated with pH 7.4 HEPES buffer, to separate the liposomes from non-transferred micellar PL and free antibody. The antibody incorporation ranged from 25 to 40 μg Ab/μmol liposome PL.

2.8. In vitro binding and uptake of immunoliposomes

Binding experiments were performed as previously described [7]. Liposomes of different formulations, including non-targeted Stealth liposomes (SL) and anti-CD19-targeted liposomes made by conventional techniques (SIL[anti-CD19]) or post-insertion techniques (PIL[anti-CD19]), were prepared with 55.5 kBq of [^{3}H]CHE per μmol PL. Namalwa cells (1×10^6 cells/well) were plated in a volume of 0.2 or 0.3 ml. In competition experiments, excess free anti-CD19 (3-fold at the highest PL concentration and 97-fold at the lowest) was added to the wells 20 min before the addition of SIL[anti-CD19] or PIL[anti-CD19]. Control immunoliposomes were made using an isotype-matched control antibody substituted for the anti-CD19. The cells were incubated for 1 h at 37°C and the [^{3}H]CHE counts associated with the cells were determined after washing three times with phosphate-buffered saline. These data were transformed into pmol PL uptake per 10^6 cells using the specific activity. Three replicates of binding data were used to generate a binding curve and the B_{max} and K_d values were determined by non-linear regression using GraphPad Prism software (San Diego, CA).

2.9. Cytotoxicity experiments

The cytotoxicities of free DXR, or doxorubicin loaded into non-targeted liposomes (DXR-SL), or targeted liposomes (DXR-SIL[anti-CD19] or DXR-PIL[anti-CD19]) was determined for Namalwa cells using the MTT assay [23]. The procedure has been previously described [7]. 5×10^4 Namalwa cells were plated in 96-well, round bottom plates in a volume of 0.1 ml. The cells were exposed to drug for either 1 or 24 h.

2.10. Pharmacokinetics

For pharmacokinetics (PK) determinations, liposomes were loaded with ^{125}I-TI and experiments were performed as previously described [7]. For the targeted formulations, either sheep IgG or anti-CD19 antibodies were coupled to the liposomes. The studies were carried out in either naive (no tumor) Balb/C cr Alt BM mice or in SCID mice inoculated i.v. with 5×10^6 cells Namalwa cells in 0.2 ml at 24 h prior to initiation of the PK studies. Pharmacokinetic parameters were calculated using a polyexponential curve stripping and least squares parameter estimation program, PKAnalyst Software (Micromath, Salt Lake City, UT).

2.11. Therapeutic efficacy

The therapeutic efficacies were compared in SCID mice inoculated i.v. with 5×10^6 cells Namalwa cells, as previously described [7]. Treatments were given at 24 h post inoculation and consisted of saline controls, free DXR, DXR-SL, DXR-SIL[anti-CD19] or DXR-PIL[anti-CD19]. The mice were dosed at 2.5 mg DXR/kg according to the mean weight of each treatment group. The mice were monitored daily and euthanized at the onset of hind leg paralysis (HLP), or upon reaching a moribund state.

2.11. Statistical analysis

Comparisons of binding, cytotoxicity, pharmacokinetics and therapeutic efficacies were done using a one-way analysis of variance (ANOVA) with GraphPad Instat Software, version 3.0 (San Diego, CA). The Tukey post-test was used to compare the different treatment means and P-values less than 0.05 were considered significant. The K_d and B_{max} for SIL[anti-CD19] and PIL[anti-CD19] were statistically compared using an unpaired t-test and GraphPad Prism software.

3. Results

3.1. In vitro binding and uptake

The radiolabeled counts associated with the cells reflect a combination of binding to cell surface CD19 epitopes and receptor-mediated internalization of the liposomes. In vitro binding and uptake of SL, SIL[anti-CD19] or PIL[anti-CD19] by Namalwa cells is shown in Fig. 1. As expected, the non-specific absorption of SL to Namalwa cells increased linearly with increasing concentrations of PL (Fig. 1A). The association of SIL coupled to a non-specific, isotype-matched antibody was not different from that observed for SL (Fig. 1). For the targeted formulations at a PL concentration of 400 nmol/ml, the total binding and uptake for SIL[anti-CD19] or PIL[anti-CD19] were 6.0-fold or 5.0-fold greater than SL, respectively ($P < 0.001$) (Fig. 1A). The specific binding and uptake of PIL or SIL saturated above PL concentrations of 400 nmol/ml (Fig. 1B). No significant differences were observed between SIL and PIL. In

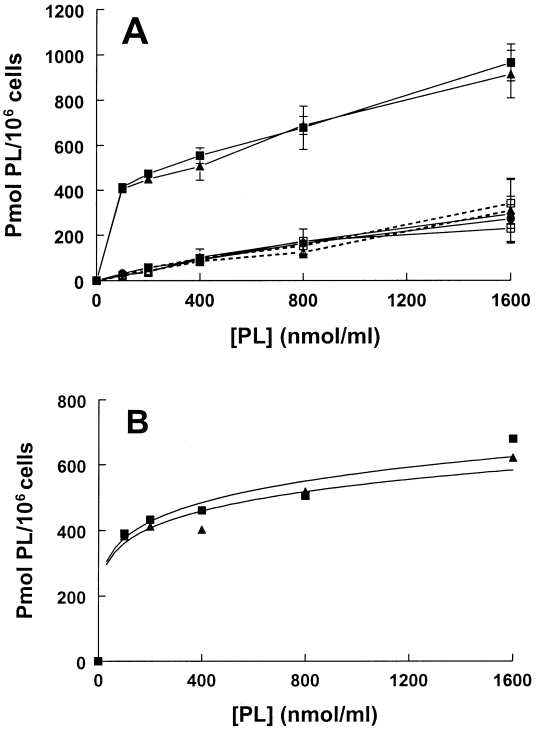

Fig. 1. Comparison of the binding and uptake of non-targeted liposomes with anti-CD19-targeted liposomes. Liposomes were composed of HSPC:CHOL:mPEG$_{2000}$-DSPE, at a molar ratio of 2:1:0.1 (100 ± 10 nm in diameter) and labeled with [^{3}H]CHE. Targeted formulations contained 25–40 μg anti-CD19/μmol PL. Increasing concentrations of SL (●), SIL[anti-CD19] (■) or PIL[anti-CD19] (▲) ($n = 3$) were incubated with 1×10^6 Namalwa cells for 1 h at 37°C. Isotype-matched control preparations of SIL[IgG2a] (□, solid line) or PIL[IgG2a] (△, solid line) were also examined. In competition experiments 3–97-fold excess free anti-CD19 was incubated with the cells at 20 min before the addition of SIL[anti-CD19] (□, dashed line) or PIL[anti-CD19] (△, dashed line) ($n = 6$). (A) Total cell-associated PL; (B) specific binding and uptake for SIL[anti-CD19] or PIL[anti-CD19]. Data are expressed as pmol PL/10^6 cells ± S.D.

Table 1
Cytotoxicity of non-targeted and anti-CD19-targeted formulations of DXR against CD19$^+$ Namalwa cells

Formulation	IC_{50} (μM DXR), 1 h (n = replicates)	IC_{50} (μM DXR), 24 h (n = replicates)
Free DXR	0.6 ± 0.3 ($n = 3$)	0.3 ± 0.1 ($n = 3$)
DXR-SL	142.0 ± 27 ($n = 3$)	5.1 ± 1.3 ($n = 4$)
DXR-SIL[anti-CD19]	35 ± 25 ($n = 3$)	2.8 ± 0.7 ($n = 4$)
DXR-PIL[anti-CD19]	31 ± 8.9 ($n = 4$)	2.8 ± 0.5 ($n = 3$)

Namalwa cells (5×10^5) were incubated with various liposome formulations (six wells each) for 1 or 24 h at 37°C in an atmosphere of 5% CO_2 and 90% humidity. The liposomes were composed of HSPC:CHOL:mPEG$_{2000}$-DSPE (2:1:0.1, mol/mol) and targeted formulations were coupled to 25–40 μg anti-CD19/μmol PL using the Mal-PEG coupling method. Each plate was incubated for a total of 48 h, after which an MTT assay was performed. The data are expressed as mean IC_{50} in μM ± S.D. for three or four separate replicates (n) of the MTT assay.

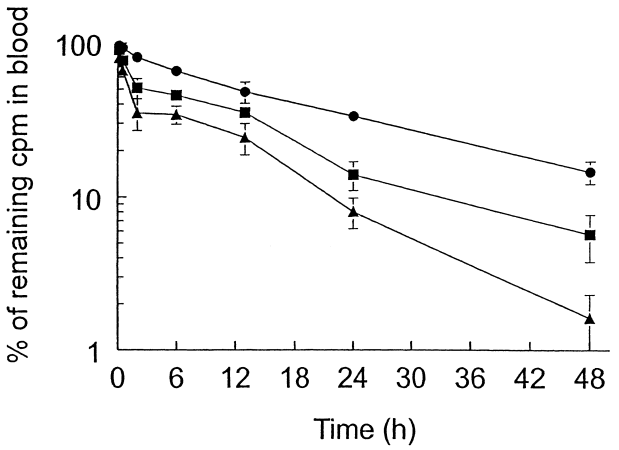

Fig. 2. Blood clearance of targeted versus non-targeted liposomes in mice. Mice (Balb/C cr Alt BM) were injected i.v. via the tail vein with a single bolus dose of 0.5 μmol liposome PL. Liposomes were composed of HSPC:CHOL:mPEG$_{2000}$-DSPE (2:1:0.1, mol/mol, 100 ± 10 nm) and loaded with the aqueous space marker ^{125}I-TI. Formulations included SL (●), SIL[anti-CD19] (■), and PIL[anti-CD19] (▲). Targeted formulations were coupled to 25–40 μg Ab/μmol PL. Data are expressed as the % of cpm in blood of counts remaining in the body at each time point (mean ± S.D., $n = 3$).

competition experiments the specific binding of both SIL[anti-CD19] and PIL[anti-CD19] was inhibited and binding and uptake levels became similar to those of SL (Fig. 1A).

The number of binding sites (B_{max}) and the K_d (± S.E.) were determined for the two targeted formulations. The B_{max} was found to be 604 ± 71 pmol/1 000 000 cells for SIL[anti-CD19] and 568 ± 64 pmol/1 000 000 cells for PIL[anti-CD19]. There was no significant difference between B_{max} for each of the two targeted formulations. Similarly, there was no significant difference between the K_d for SIL[anti-CD19] of 83 ± 48 μM and that of PIL[anti-CD19] of 79 ± 44 μM.

The number of liposomes per μmol PL was calculated from the literature values for bilayer thickness and the molecular areas for HSPC, CHOL, and PEG-DSPE. Assuming that the liposomes were spherical, 100 nm in diameter, and contained unilamellar bilayers with monodisperse PL, the number of liposomes per μmol PL is estimated at 7.7×10^{12}. From this information the number of antibodies for liposomes containing 25–40 μg anti-CD19/μmol PL was calculated to range between 13 and 21 antibodies per liposome. Using these calculations, the B_{max} for SIL[anti-CD19] and PIL[anti-CD19] translate into approx. 4654 and 4372 liposome binding sites per cell, respectively.

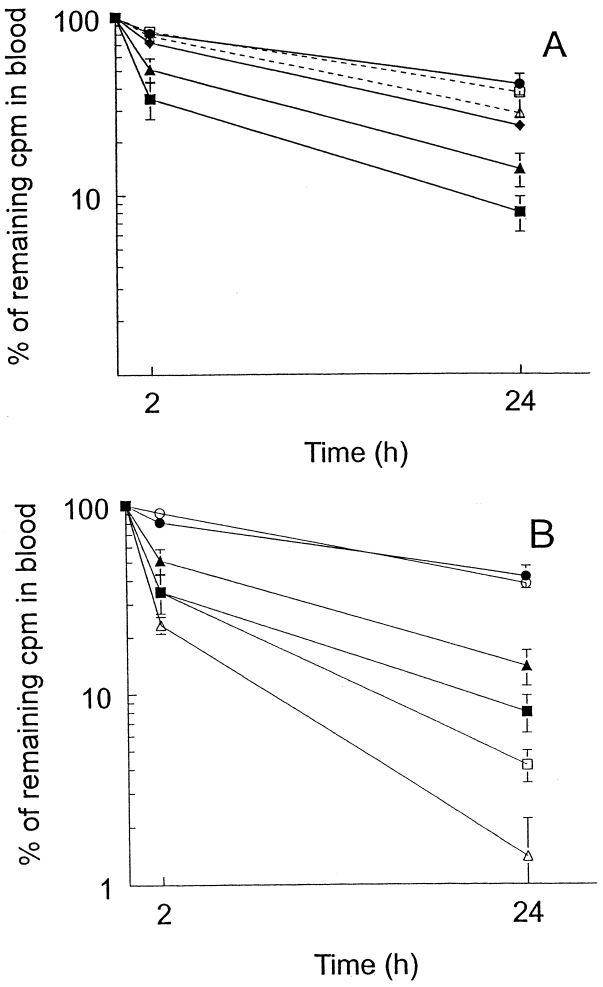

Fig. 3. Clearance of liposomes as a function of antibody, coupling method or presence of tumor cells. Mice were injected i.v. via the tail vein with a single bolus dose of 0.5 μmol liposomal PL. Liposomes were composed of HSPC:CHOL:PEG$_{2000}$-DSPE (2:1:0.1, mol/mol, diameter 100 ± 10 nm) and loaded with the aqueous space marker ^{125}I-TI. Targeted formulations were coupled to 25–40 μg Ab/μmol PL using the Mal-PEG method unless otherwise indicated. (A) Clearance in naive (no tumor) BALB/c cr Alt BM mice as a function of the targeting Ab and coupling method. ●, SL; ▲, SIL[anti-CD19]; ◆, Hz-PEG-SIL[anti-CD19]; ■, PIL[anti-CD19]; △, SIL[Sheep IgG]; □, PIL[sheep IgG]. (B) Clearance of SL or anti-CD19 immunoliposomes in naive BALB/c cr Alt BM mice (closed symbols) vs. SCID mice inoculated with 5×10^6 Namalwa cells 24 h prior to liposomes (open symbols). ●,○, SL; ▲,△, SIL[anti-CD19]; ■,□, PIL[anti-CD19]. Data are expressed as the % cpm in blood of counts remaining in the body at each time point (mean ± S.D., $n = 3$).

3.2. Cytotoxicity

The average in vitro IC_{50} values for free DXR, DXR-SL, DXR-SIL[anti-CD19] or DXR-PIL[anti-CD19] for several cytotoxicity assays are shown in Table 1. Free doxorubicin was significantly more cytotoxic than DXR-SL, DXR-SIL[anti-CD19] or DXR-PIL[anti-CD19] for the 1 h incubation ($P < 0.001$) and the 24 h incubation ($P < 0.05$ to $P < 0.001$). Targeted formulations were significantly more cytotoxic than non-targeted formulations ($P < 0.001$) but not significantly different from each other ($P > 0.05$).

3.3. Pharmacokinetics

The clearance profiles for ^{125}I-TI-loaded SL, SIL[anti-CD19] or PIL[anti-CD19] in BALB/c mice are shown in Fig. 2. Both of the targeted formulations were cleared significantly more rapidly than SL. The clearance profiles of the targeted formulations were characterized by an early rapid phase of clearance. Although PIL appeared to be removed more rapidly than SIL, statistical comparison of the two suggested that the difference barely reached significance ($P < 0.05$).

As the source of antibody, as well as the coupling method might affect clearance, a comparison was made of the clearance rates for immunoliposomes for different antibodies and coupling methods and in tumor-bearing versus non-tumor-bearing mice (Fig. 3). The clearance kinetics for SIL or PIL coupled to sheep IgG were not different from the clearance kinetics of SL (Fig. 3A). Liposomes coupled to anti-CD19 by the Mal-PEG method were cleared more rapidly than liposomes coupled to sheep IgG by the same method and PIL[anti-CD19] and were cleared more rapidly than SIL[anti-CD19], although this was barely statistically significant. Interestingly, SIL[anti-CD19] coupled by the Mal-PEG method were cleared more rapidly than similar liposomes prepared by a coupling method that results in a hydrazone bond between the Fc region of the antibody and the PEG [7]. The terminal half-lives ($t_{1/2\beta}$) for SL, SIL[sheep IgG], PIL[sheep IgG], SIL[anti-CD19] or PIL[anti-CD19] were 21.8, 15.5, 17.7, 16.4, and 17.4 h, respectively (data not shown). In all cases the volume of distribution, V_D, closely approximated the blood volume (data not shown).

Since the clearance of anti-CD19-targeted liposomes is expected to be altered in tumor-bearing mice, the clearance of PIL[anti-CD19] or SIL[anti-CD19] was evaluated in SCID mice injected i.v. with Namalwa cells, which is the same animal model used to evaluate the therapeutic efficacy. As expected, the clearance of the targeted liposomes, but not the non-targeted liposomes, was more rapid in tumor-bearing SCID mice than in conventional Balb/c mice (Fig. 3B). Two hours post injection only 25–35% of the administered dose remained in blood for PIL[anti-CD19] or SIL[anti-CD19] in tumor-bearing mice.

3.4. In vivo therapeutics

Table 2 shows the mean survival times (MST) and % increased life spans (ILS) for mice treated with saline, free DXR, DXR-SL, DXR-SIL[anti-CD19] or PIL[anti-CD19]. There were no significant differ-

Table 2
Therapeutic efficacy of non-targeted and targeted formulations of DXR in SCID mice implanted with human B-lymphoma cells

Formulation	MST ± S.D. (days)	ILS (%)
Saline control ($n = 6$)	28.2 ± 2.1	–
Free DXR ($n = 5$)	31.0 ± 3.7	9.9
DXR-SL ($n = 5$)	29.8 ± 2.6	5.7
DXR-SIL[anti-CD19] ($n = 7$)	38.4 ± 4.2	36.2
DXR-PIL[anti-CD19] ($n = 5$)	36.6 ± 3.2	29.8

SCID mice received i.v. Namalwa cells (5×10^6 cells in 0.2 ml) 24 h before a single treatment with 2.5 mg/kg DXR. Liposomes were composed of HSPC:CHOL:mPEG-DSPE (2:1:0.1, mol/mol, 100 ± 10 nm) with or without 25 μg anti-CD19/μmol liposome PL, coupled to the PEG terminus by the Mal-PEG method. Doxorubicin was loaded into liposomes by the ammonium sulfate gradient method at 0.2 mg DXR/mg PL. MST denotes mean survival time and ILS denotes increased life span ($n = 5$).

ences in the MST for saline, free DXR or DXR-SL. However, both targeted formulations showed significantly increased MST compared to the other formulations ($P < 0.05$ to $P > 0.001$). No significant differences were observed between DXR-PIL[anti-CD19] and SIL[anti-CD19].

4. Discussion

In this paper the in vitro and in vivo binding, cytotoxicity and therapeutic effects of anti-CD19 immunoliposomes made by the post-insertion technique were compared to those of immunoliposomes made by a conventional coupling technique using a human B-lymphoma model. In terms of the assay results, there was little to choose between the two methods for preparing immunoliposomes. However, in terms of their ease and speed of preparation and their flexibility, PIL would be the clear favorite for use in manufacturing immunoliposomes for clinical applications.

The results from the binding and competition experiments support a conclusion that, in the case of both SIL[anti-CD19] and PIL[anti-CD19], the antibody mediated a specific targeting effect. In addition, these experiments and previous experiments in our laboratory using non-specific isotype control antibodies have demonstrated that this effect is specific to anti-CD19 [7,24]. Further, the K_d and B_{max} for both preparations were similar.

Interestingly, the estimated number of binding sites for the anti-CD19 immunoliposomes was approx. 7-fold lower than that previously reported [7] and was also lower than the number of sites reported for free anti-CD19 mAb (HD37) [25]. The reason for this disparity may be related to differences in the coupling method between these and previous results. In the previous study, the hydrazide coupling method was employed [7]. This method, which couples antibodies to the PEG terminus through their Fc region, results in the attachment of antibodies in a consistent orientation that leaves the antigen-binding region exposed and able to interact with the target. The coupling method employed in this study (Mal-PEG) results in random thiolation of the antibody and therefore random orientation of the antibody on the liposome. This may result in screening or blocking of the binding region of the antibody and an apparent reduction in the number of binding sites. In addition, the introduction of sulfhydryl groups to amino acids within the antigen-binding region of the antibody by Traut's reagent could interfere with binding. Indeed, antibody activated with Traut's reagent has been shown to bind less effectively to Namalwa cells than non-treated antibody (Allen laboratory, unpublished results). Further, while small changes in the antigen-binding region may not prevent binding of the anti-CD19 antibody to the CD19 epitope, it is possible that receptor activation could be blocked, leading to decreased levels of receptor-mediated endocytosis and decreased receptor recycling (recall that the binding results are a sum of both binding and uptake). The Mal-PEG coupling method was originally described for the coupling of antibody fragments to liposomes [18]. Since Fab′ fragments can be easily coupled to lipids via naturally occurring inter-chain sulfhydryl groups, there is no need for thiolation of the antibody. Preliminary results from our laboratory suggest that SIL[anti-CD19] made with Fab′ fragments rather than whole antibody have improved binding and uptake by Namalwa cells (manuscript in preparation). This further suggests that the antibody binding may be compromised by thiolation.

Overall, the cytotoxicity results were in agreement with the previous findings by Lopes de Menezes et al. [7] and no differences between PIL[anti-CD19] and SIL[anti-CD19] were observed. Since there was no significant difference in the B_{max} and K_d for either of the two targeted formulations, it is likely that the equivalent cytotoxicity results by a similar mechanism of drug delivery to the target cells, probably by receptor-mediated endocytosis of intact liposomes. The targeted formulations were expected to have a cytotoxic advantage due to receptor-mediated endocytosis of the drug-loaded liposomes. Intracellular delivery of drug-loaded liposomes is thought to increase drug exposure, provided that the drug is released from the endosome–lysosome compartment [22]. Conversely, the cytotoxicity of DXR-SL is dependent on the release of DXR from the liposomes, which occurs slowly. Hence the very low cytotoxicity of DXR-SL for short incubation times was not surprising. At longer time points, release of drug from DXR-SL would be higher and the differences be-

tween non-targeted and targeted formulations should decrease, as we observed.

Because the post-insertion technique involves exposing the antibody to elevated temperature (60°C) for 1 h, the potential exists for detrimental effects on the antibody that could reduce its binding affinity and/or avidity for its target antigen. Since no significant differences were observed between PIL and SIL in binding, cytotoxicity or therapeutic benefit, the antibody appears to be stable at this temperature over this incubation time.

Both targeted formulations were cleared more rapidly than the non-targeted formulations in naive, immune-competent mice, likely due to the binding of liposomes to CD19-expressing normal B-cells in the Balb/c mice. This explains the increased rate of clearance of anti-CD19 immunoliposomes compared to sheep IgG immunoliposomes. It also suggests that the behavior of immunoliposomes in vivo may be subject to antibody- or model-specific effects and the results reported in this study cannot necessarily be extended to other antibodies or other coupling methods. For example, in this study the rate of clearance of SIL[anti-CD19] coupled by the Mal-PEG method was faster than previously reported for SIL[anti-CD19] made by the Hz-PEG coupling method [7]. In our current study, a direct comparison of SIL[anti-CD19] prepared by the Hz-PEG vs. Mal-PEG methods showed an increased rate of clearance for the latter, despite equivalent antibody densities. Since the hydrazide coupling method is site-directed to the Fc region of the antibody, clearance of the immunoliposomes by Fc receptor-mediated mechanisms will be substantially reduced relative to the Mal-PEG method where the Fc region of the antibody may be exposed on some proportion of the antibody population. Overall, this finding suggests that the Mal-PEG coupling method would be more beneficially applied to Fab′ or scFv fragments that lack the Fc portion of the antibody. Preliminary work in our laboratory has shown that SIL[anti-CD19 Fab′] prepared using the Mal-PEG method are cleared much less rapidly than SIL[anti-CD19] (whole antibody). For example, at 24 h post injection 30% of SIL[anti-CD19 Fab′] remained in blood compared to only 3% of SIL[anti-CD19] (manuscript in preparation).

Although there was a tendency for PIL to be cleared more rapidly than SIL, this was barely significant and could have been due to small variations in the numbers of antibodies at the liposome surface since the pharmacokinetics is sensitive to antibody density. Although every attempt was make to match the antibody densities in samples, it is impossible to do this exactly. Although we have no evidence for this as yet, there may also be differences in the orientation of the antibody during the coupling procedure when coupling is done with micelles as opposed to whole liposomes. This might result in changes in the degree of exposure of the binding site region or the Fc region of the antibody that might affect the pharmacokinetics.

It would be desirable if the clearance of the targeted formulations were slower than reported here. However, since binding and internalization in vitro are rapid (within a few minutes), the circulation half-lives of the immunoliposomes should be long enough to allow in vivo binding and uptake leading to a therapeutic effect. Indeed, mice treated with SIL[anti-CD19] and PIL[anti-CD19] had significantly increased survival times compared to free drug or non-targeted liposomes, and there was no significant difference between the two targeted formulations. The therapeutic advantage of anti-CD19 immunoliposomes has been previously shown to be specific to anti-CD19 and to require the presence of DXR in the liposomes [7]. In other words, the cytotoxic effect of anti-CD19 antibody is not primarily responsible for the therapeutic effect [7,26].

Given that the pharmacokinetics for SIL[anti-CD19] and PIL[anti-CD19] prepared by the Mal-PEG coupling method were less favorable than the pharmacokinetics previously reported for SIL[anti-CD19] prepared by the Hz-PEG method [7], it might be expected that the therapeutic efficacy would decrease. Using an identical model, Lopez de Menezes et al. reported an ILS of 60% (versus an ILS of 36.2% in our study) for mice treated with a slightly higher dose, 3 mg/kg DXR-SIL[anti-CD19] (versus 2.5 mg/kg in our study), at the same tumor cell burden, route of injection and time of treatment post inoculation [7]. The decrease in dose, the decreased binding efficacy due to random orientation of the antibody, as well as the more rapid clearance kinetics are likely responsible for the poorer response.

This study shows that the post-insertion approach is amenable to the preparation of CD19-targeted im-

munoliposomes, loaded with doxorubicin by the ammonium sulfate method. However, for this approach to be widely applicable to the manufacture and administration of targeted liposomes, it is necessary to demonstrate that the post-insertion approach is widely applicable to the preparation of targeted liposomes using other antibodies, antibody fragments, peptides or other ligands as well as other drugs. Nevertheless, it would appear that the post-insertion approach to the formulation of immunoliposomes has the necessary ease, speed and flexibility of production and the therapeutic efficacy that makes it useful from the manufacturing perspective, as well as the clinical perspective, for improving the selective toxicity of anticancer or other drugs.

Note added in proof

A recent paper (M. Sugano, J.K. Egilmez, S.J. Yokota, F.-A. Chen, J. Harding, S.K. Huang, R.B. Bankert, Cancer Res. 60 (2000) 6942–6949) used the post-insertion technique to insert Fab′-antibody fragments into preformed liposomal doxorubicin and these were used, with good therapeutic efficacy, in a human lung tumor xenograft model in SCID mice.

Acknowledgements

We thank Tatsuhiro Ishida for his expert advice on the formation of the PIL. We also thank Susan Cubitt for technical assistance and Elaine Moase for technical assistance and for critical review of the manuscript. This work was supported by the Canadian Institutes of Health Research (MT-9127) and by Alza Corporation.

References

[1] R.J. Debs, T.D. Heath, D. Papahadjopoulos, Biochim. Biophys. Acta 901 (1987) 183–190.
[2] I. Ahmad, M. Longenecker, J. Samuel, T.M. Allen, Cancer Res. 53 (1993) 1484–1488.
[3] D. Goren, A.T. Horowitz, S. Zalipsky, M.C. Woodle, Y. Yarden, A. Gabizon, Br. J. Cancer 74 (1996) 1749–1756.
[4] J.W. Park, K. Hong, D.B. Kirpotin, O. Meyer, D. Papahadjopoulos, C.C. Benz, Cancer Lett. 118 (1997) 153–160.
[5] K. Maruyama, T. Takizawa, N. Takahashi, T. Tagawa, K. Nagaike, M. Iwatsuru, Adv. Drug Deliv. Rev. 24 (1997) 235–242.
[6] R.J. Lee, P.S. Low, J. Liposome Res. 7 (1997) 455–466.
[7] D.E. Lopes de Menezes, L.M. Pilarski, T.M. Allen, Cancer Res. 58 (1998) 3320–3330.
[8] Y. Tseng, R. Hong, M. Tao, F. Chang, Int. J. Cancer 80 (1999) 723–730.
[9] D. Goren, A.T. Horowitz, D. Tzemach, M. Tarshish, S. Zalipsky, A. Gabizon, Clin. Cancer Res. 6 (2000) 1949–1957.
[10] J.A. Reddy, P.S. Low, J. Control. Release 64 (2000) 27–37.
[11] T. Ishida, D.L. Iden, T.M. Allen, FEBS Lett. 460 (1999) 129–133.
[12] P.S. Uster, T.M. Allen, B.E. Daniel, C.J. Mendez, M.S. Newman, G.Z. Zhu, FEBS Lett. 386 (1996) 243–246.
[13] T.M. Allen, C.B. Hansen, S. Zalipsky, in: D.D. Lasic, F. Martin (Eds.), Stealth Liposomes, CRC Press, Boca Raton, FL, 1995, pp. 233–244.
[14] T.M. Allen, C.B. Hansen, F. Martin, C. Redemann, A. Yau-Young, Biochim. Biophys. Acta 1066 (1991) 29–36.
[15] S. Zalipsky, Bioconjugate Chem. 4 (1993) 296–299.
[16] E.F. Sommerman, P.H. Pritchard, P.R. Cullis, Biochem. Biophys. Res. Commun. 122 (1984) 319–324.
[17] H. Zola, P.J. Macardle, T. Bradford, H. Weedon, H. Yasui, Y. Kurosawa, Immunol. Cell Biol. 69 (1991) 411–422.
[18] D. Kirpotin, J.W. Park, K. Hong, S. Zalipsky, W.-L. Li, P. Carter, C.C. Benz, D. Papahadjopoulos, Biochemistry 36 (1997) 66–75.
[19] G. Haran, R. Cohen, L.K. Bar, Y. Barenholz, Biochim. Biophys. Acta 1151 (1993) 201–215.
[20] E.M. Bolotin, R. Cohen, L.K. Bar, S.N. Emanuel, D.D. Lasic, Y. Barenholz, J. Liposome Res. 4 (1994) 455–479.
[21] G.R. Bartlett, J. Biol. Chem. 234 (1959) 466–468.
[22] D.E. Lopes de Menezes, M.J. Kirchmeier, J.-F. Gagne, L.M. Pilarski, T.M. Allen, J. Liposome Res. 9 (1999) 199–228.
[23] T. Mosmann, J. Immunol. Methods 65 (1983) 55–63.
[24] D.E. Lopes de Menezes, L.M. Pilarski, A.R. Belch, T.M. Allen, Biochim. Biophys. Acta 1466 (2000) 205–220.
[25] V.S. Goldmacher, C.F. Scott, J.M. Lambert, G.D. McIntyre, W.A. Blattler, A.R. Collinson, S.A. Cook, H.S. Slayter, E. Beaumont, S. Watkins, J. Cell. Physiol. 141 (1989) 222–234.
[26] M.A. Ghetie, L.J. Picker, J.A. Richardson, K. Tucker, J.W. Uhr, E.S. Vitetta, Blood 83 (1994) 1329–1336.